Buckling of graphene under compressive strain: DFT calculations and second generation REBO potential

C. Chil, J. Durinck, C. Coupeau

▶ **To cite this version:**

C. Chil, J. Durinck, C. Coupeau. Buckling of graphene under compressive strain: DFT calculations and second generation REBO potential. Extreme Mechanics Letters, 2022, 56, pp.101845. 10.1016/j.eml.2022.101845 . hal-03826914

HAL Id: hal-03826914
https://hal.science/hal-03826914

Submitted on 16 Apr 2024

HAL is a multi-disciplinary open access archive for the deposit and dissemination of scientific research documents, whether they are published or not. The documents may come from teaching and research institutions in France or abroad, or from public or private research centers.

L'archive ouverte pluridisciplinaire **HAL**, est destinée au dépôt et à la diffusion de documents scientifiques de niveau recherche, publiés ou non, émanant des établissements d'enseignement et de recherche français ou étrangers, des laboratoires publics ou privés.

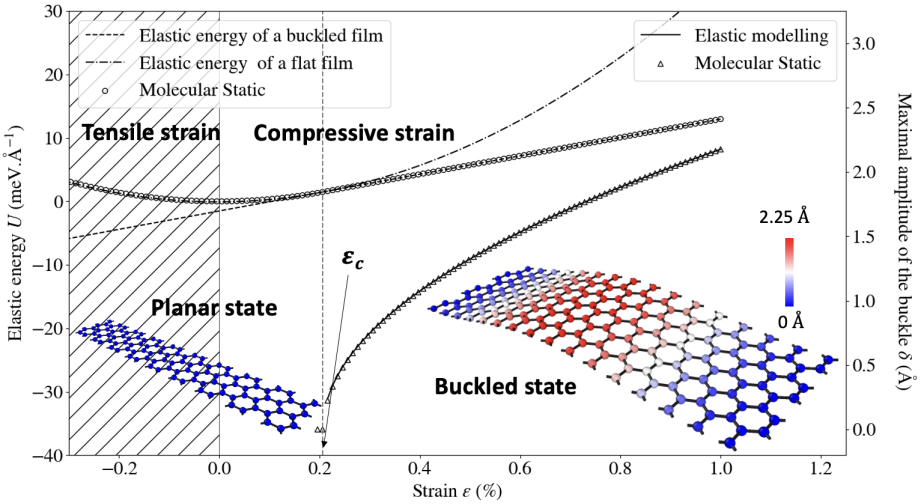

Graphical Abstract

Buckling of graphene under compressive strain: DFT calculations and second generation REBO potential

C. Chil, J. Durinck, C. Coupeau

Highlights

Buckling of graphene under compressive strain: DFT calculations and second generation REBO potential

C. Chil, J. Durinck, C. Coupeau

- Buckling of graphene has been investigated using DFT calculations and MS simulations.
- A constant value for the effective thickness of graphene has been determined whatever the size of the buckle.
- No orientation (armchair/zigzag) effect of graphene on buckling.

Buckling of graphene under compressive strain: DFT calculations and second generation REBO potential

C. Chil[a], J. Durinck[a], C. Coupeau[a]

[a]*Institut Pprime, Université de Poitiers/UPR 3346 CNRS/ENSMA, France*

Abstract

Mechanical properties of coatings can be determined from the characterization of the buckling structures morphologies. Extending this scientific strategy to 2D materials has been proposed by defining an effective thickness that only depends on the elastic coefficients. In this context, the buckling of graphene under compressive strain is studied by first-principles calculations and molecular statics simulations. No effect of the graphene orientation (armchair or zigzag) with respect to the straight-sided buckle is evidenced on the morphology of buckles. The results confirm also that the effective thickness stays constant whatever the size of the buckles, even at the nanometer scale.

Keywords: Buckling, Graphene, Density Functional Theory, Molecular Statics

1. Introduction

High compressive stresses are often observed in coatings and thin films (see [1] for a review). They are then prone to delaminating and buckling, a phenomenon that leads in most cases to the loss of functionality that was initially conferred to the film/substrate composites. The elementary buckling structures observed experimentally most often consist in telephone cords, circular blisters or straight-sided buckles [2–14]. The buckling of coatings has been theoretically studied in the past, mainly in the framework of the elastic theory of thin plates. In particular, the Föppl-von Kármán (FvK) equations allow determining the equilibrium shape of the buckled structure and the critical strain (or stress) for buckling to occur [15, 16]. Finite element simulations have been also extensively carried out to figure out the

influence of different physical parameters on buckling, such as the pressure mismatch between the inner and outer parts of the buckle [12, 17, 18] or the elastic contrast between the film and the substrate [19, 20], the plasticity of the film and the substrate as well [18, 21, 22]. Based on these elastic models, a new scientific strategy has been thus developed over the last decade, that consists in determining, from a fine morphological characterization of elementary buckles, some mechanical parameters of the involved coated systems, such as the Young's modulus, the internal stresses or the film/substrate adhesion [3, 4, 7, 10, 22–25].

Buckling structures have already been experimentally observed in 2D materials. For instance, networks of straight-sided buckles are commonly evidenced by scanning probe microscopy on graphene grown by chemical vapor deposition (CVD) on different types of substrates, such as SiC(0001) [24], poly-ethylene-terephthalate (PET) [26, 27] or cobalt [28]. More complex structures are sometimes observed, such as for instance multi-lobed buckles on Ir(111) not really well-understood up to now [29] or even bubbles on exfoliated graphene deposited on silicon oxide [30]. Using the previously mentioned scientific strategy to determine mechanical properties from buckles morphology may be questionable since the thickness of a 2D material is not explicitly defined. Molecular dynamics (MD) simulations have been carried out to highlight the mechanical behaviour of graphene under stress. A non geometrical thickness, called effective thickness in the following, has thus been determined and found to depend on both the bending and in-plane stiffness [31–33]. Most of the MD studies have been based on carbon nanotubes (CNTs) and the elastic coefficients have been found to stay roughly constant as a function of the CNT radius of curvature, up to a critical value of around 1 nm [31, 33]. Moreover, it has been demonstrated that the elastic coefficients at such an atomic scale sometimes depend [31] or not [33, 34] on the armchair or zigzag configurations of graphene. These numerical MD results, however, depend significantly on the interatomic potentials that are used to describe the mechanical behaviour of graphene. Many density functional theory (DFT) calculations have been reported in the literature but, to our knowledge, no DFT studies have been specifically focused on the buckling of graphene sheets. It can be however noted that MD simulations have been performed on graphene by Lu and Huang [34] who have shown in particular that the critical strain for buckling linearly increases with the decreasing width of the buckle, suggesting that the elastic theory is still valid for such a 2D material.

In this context, we have performed DFT calculations and molecular statics (MS) simulations on single layer graphene strained by uniaxial compression. The numerical results are first presented and then compared and discussed with respect to other previous studies in which values of the graphene thickness have been determined. The relevance of experimentally characterizing the morphology of buckles to extract some mechanical information on 2D materials is finally discussed.

2. Numerical details

The two representative graphene monolayers considered in the simulations are shown in Fig. 1: one with the armchair direction (Fig. 1a) and the other with the zigzag (Fig. 1b) lying along the (Ox) direction. Periodic boundary conditions are implemented along (Ox), (Oy) and (Oz) directions. The dimension L_x is ranging from 5 to 43 unit cells and the dimension L_y is fixed to 3 unit cells each composed by 4 atoms. L_z is equal to 15 Å, leaving a sufficiently thick vacuum layer that prevents the graphene from self-interacting with its image along (Oz). A sinusoidal out-of-plane perturbation with a maximum deflection equal to 1 Å, located at the $L_x/2$ position, is imposed to the graphene. The strain is then applied by increments of 0.01 % along the (Ox) axis, *i.e.* along either the armchair or the zig-zag directions. At each strain step, the different atomic configurations are released using DFT calculations or MS simulations using interatomic potentials.

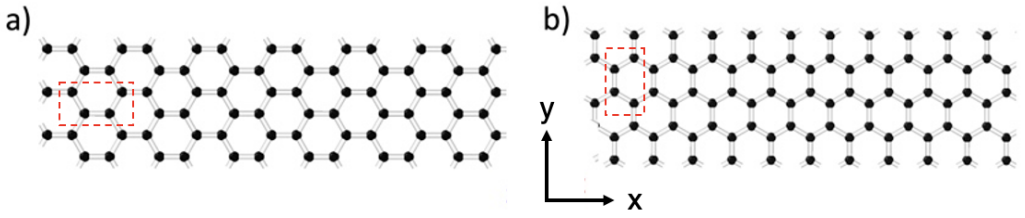

Figure 1: Atomic graphene configurations for (a) the armchair and (b) the zigzag orientations. The strain ϵ is applied along the (Ox) axis. The unit cell is represented by the red dotted rectangle.

DFT caculations are performed using the VASP (Vienna Ab initio Simulation Package) code, within the Generalized Gradient Approximation (GGA) framework parametrized by Perdew, Burke and Ernzerhof (PBE) [35]. The

interactions between ions (core electrons and atom nucleus) and valence electrons are described by the Projector Augmented Wave (PAW) pseudopotential formalism. A Monkhorst-Pack sampling of the irreducible Brillouin zone of $10\times10\times1$ is used with a kinetic cut-off energy equal to 600 eV. The groundstate charge density is calculated using the blocked Davidson iteration scheme, until the total energy no longer varies by more than 10^{-6} eV and the position of the ions is optimized according to a conjugate gradient algorithm until the maximum force on ions is less than 10^{-4} eV.Å^{-1}.

For larger graphene monolayers, with L_x ranging from 18 Å to 104 Å, molecular statics simulations are performed using the LAMMPS program [36]. Interactions between carbon atoms are modeled using the second generation of the Reactive Empirical Bond Order (REBO 2002) potential [37]. The atomic positions are optimized and the energy is minimized for each strained configuration using a conjugate gradient algorithm until the maximum force between atoms is lower than 10^{-6} eV.Å^{-1}.

3. Results

The out-of-plane displacement w of the buckled graphene strained at 1% is plotted in Fig. 2 for both the zigzag and the armchair configurations. The buckling of "thick" films has been extensively studied in the past, by using the FvK equations [15]. For a 1D straight-sided buckle on a rigid substrate, named also as the Euler's column, the equilibrium buckled shape is characterized by the displacements u and w along (Ox) and (Oz) directions respectively [15]:

$$u(x) = \frac{\pi\delta^2}{32B}\sin\left(\frac{2\pi x}{B}\right), \quad (1)$$

$$w(x) = \frac{\delta}{2}\left[1+\cos\left(\frac{\pi x}{B}\right)\right], \quad (2)$$

with δ, the maximum deflection of the buckle and B, its half width. It is shown in Fig. 2(a) and 2(b) that the numerical MS data (circular and triangular dots for the zigzag and armchair configuration, respectively) are in good agreement with the equilibrium shape predicted by the elastic continuum theory with $B = L_x/2$.

In the following, the applied strain ϵ is considered to be positive in compression and negative in tension. The evolution of the maximum deflection

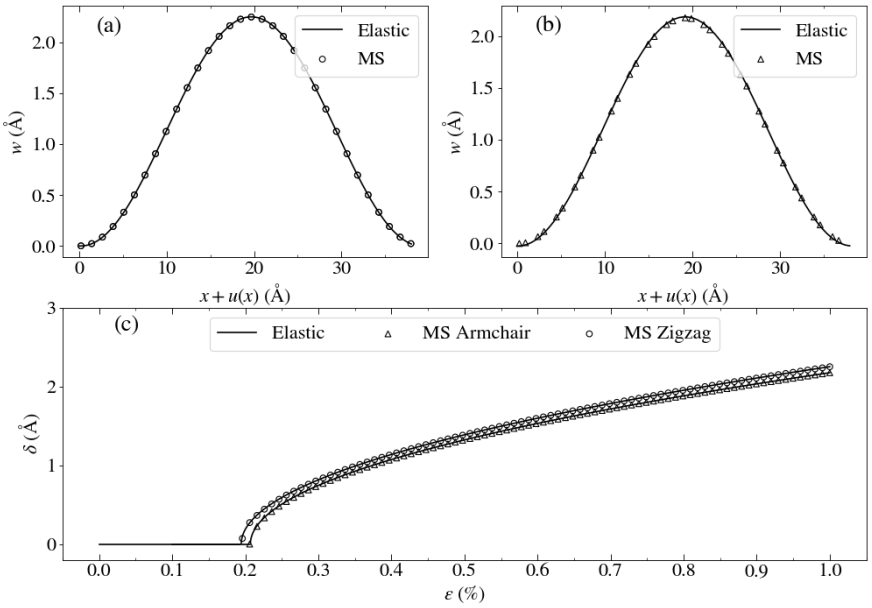

Figure 2: MS simulations of the out-of-plane displacement for (a) a zigzag ($L_x^z = 39.4\,$Å or $B_z = 19.7\,$Å, circle dots) and (b) a armchair ($L_x^a = 38.4\,$Å or $B_a = 19.2\,$Å, triangular dots) configuration. The compressive strain along the (Ox) axis is equal to 1%. The fit based on the Eq.(2) has been superimposed as straight lines. (c) Maximum deflection δ of the buckle as a function of the compressive strain ϵ, for both the armchair and zigzag configurations.

with $\epsilon > 0$ is plotted in Fig. 2(c) for the zigzag and the armchair configurations. δ continuously increases with the increasing strain for zigzag and armchair configurations. The slight difference observed in Fig. 2(c) is related to the values of half widths B_z and B_a that differ by about 0.5 Å between zigzag and armchair configurations, respectively. Finally, no buckling occurs at strain values lower than a critical strain ϵ_c. In the framework of the elastic theory, this critical strain for buckling is given, for a film with a thickness h, by [15]:

$$\epsilon_c = \frac{\pi^2}{12}\left(\frac{h}{B}\right)^2, \tag{3}$$

and the maximum deflection δ of a straight-sided buckle writes as [15]:

$$\delta = \frac{4B}{\pi}\sqrt{\epsilon - \epsilon_c}. \tag{4}$$

It is noticed in Eq.(3) that ϵ_c depends on the thickness of the film, a parameter that is not geometrically defined for graphene and for 2D materials in general. Another relationship for the critical strain can be derived from the critical load determined for the buckling of rectangular plates of width $2B$ [38]:

$$\epsilon_c = \frac{\pi^2 D}{C_{xx} B^2}, \tag{5}$$

where D is the bending modulus and C_{xx}, the in-plane elastic coefficient. Combining Eqs. (3) and (5), the expression of an effective thickness can be given by:

$$h = 2\sqrt{\frac{3D}{C_{xx}}}, \tag{6}$$

that depends only on the elastic properties of graphene. Another way to figure out the thickness of graphene is to directly use simulated data obtained for the buckling of graphene. The first method consists in fitting ϵ_c given by the Eq. (4) against the numerical values of the maximum deflection δ with respect to the applied strain ϵ. The result of the fitting procedure is shown in Fig. 2(c) as black lines, with critical strain values found equal to $\epsilon_c^a = 0.206\%$ and $\epsilon_c^z = 0.193\%$ for the armchair and zigzag directions, respectively. It is found that $\sqrt{\epsilon_c^a/\epsilon_c^z}$ is approximately equal to B_z/B_a with a relative error less than 0.7%, meaning that the buckling for both configurations behaves as predicted by the Eq. (3) with the same value of h. It confirms that the slight difference observed in Fig. 2(c) for the armchair and zigzag configurations is related to the discrepancy between half widths B_z and B_a. Another method, based on the calculation of the elastic energy stored in a strained film and already used in a previous work by Lu and Huang [34], has been considered here to systematically determine the effective thickness of graphene as a function of B for both configurations. In the planar state, the elastic energy per unit length of the film is given by [11] :

$$U_{\text{flat}} = Bh\bar{E}\epsilon^2, \tag{7}$$

where $\bar{E}$ is the reduced Young's modulus ($\bar{E} = \frac{E}{1-\nu^2}$ with ν the Poisson's

ratio). For $\epsilon > \epsilon_c$, the elastic energy per unit length of a buckled film is defined as [11]:

$$U_{\text{buckled}} = U_{\text{flat}} - Bh\bar{E}(\epsilon - \epsilon_c)^2, \tag{8}$$

leading to:

$$U_{\text{buckled}} = Bh\bar{E}\epsilon_c(2\epsilon - \epsilon_c). \tag{9}$$

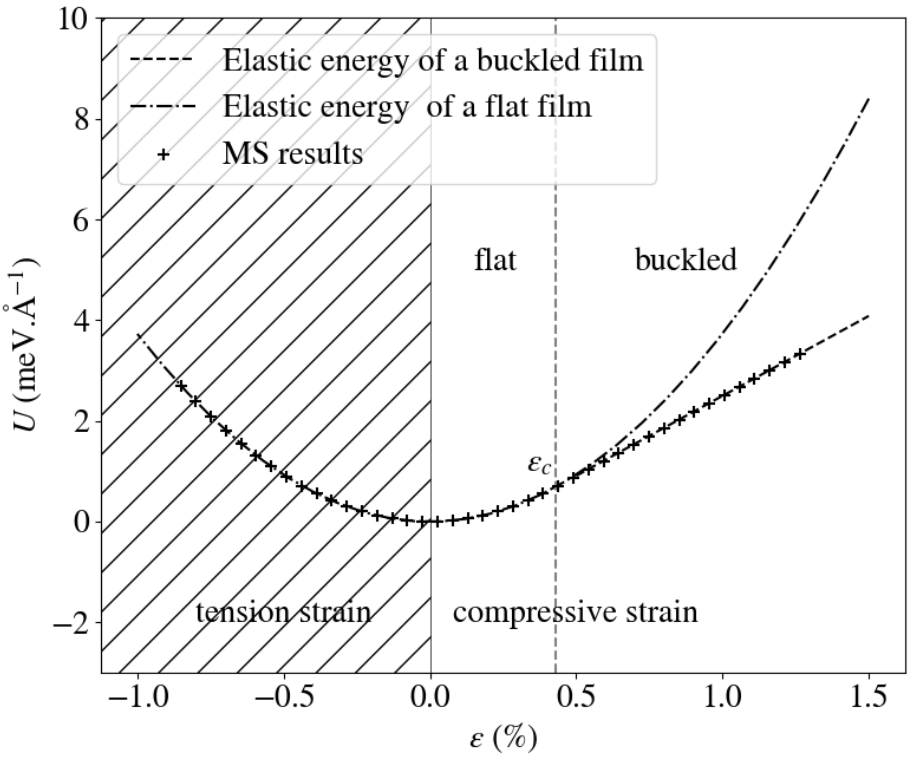

Figure 3: Energy elastic per unit length calculated by MS of a zigzag graphene (B=15 Å) as a function of the strain. The hatched zone corresponds to tension strains. Vertical dotted line corresponds to the transition between the flat (parabolic dependence) and the buckle (linear dependence) states.

Thus, the elastic energy stored in the buckled film linearly depends on ϵ, while it evolves as ϵ^2 in the planar state. These two different regimes have consequently been used to determine the buckling onset of graphene, *i.e.* at $\epsilon = \epsilon_c$. As an example, the elastic energy per length unit U extracted from

the MS simulations is plotted in Fig. 3 with respect to the applied strain ϵ, for graphene with dimensions L_x=30 Å. A critical strain ϵ_c is clearly evidenced above which the calculated elastic energy U fits with a straight line (buckled state) and below which it fits with a parabola (plate state). In this case, ϵ_c is found to be equal to 0.43%.

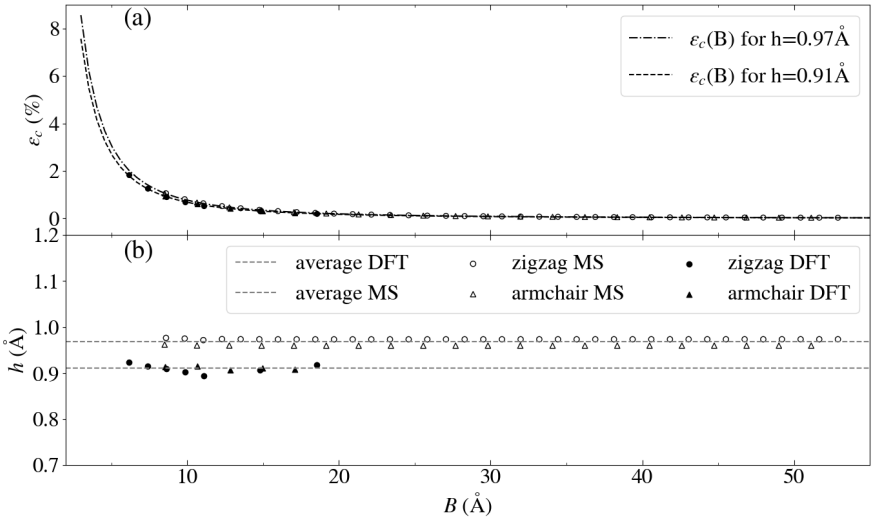

Figure 4: Critical strain for buckling ϵ_c and effective thickness h, as a function of the half-width B and for both armchair (triangular dots) and zigzag (circle dots) configurations. The MS and DFT calculations are shown in black and white dots respectively. Grey dashed lines correspond to average value for both configurations.

The critical strain ϵ_c has been determined by DFT calculations and MS simulations, for various B values ranging from 6.2 Å to 52.8 Å (Fig. 4(a)). It shows that ϵ_c continuously increases with decreasing B, in agreement with [34] and that DFT and MS calculations give similar results. The effective thickness of the graphene has been determined using the Eq.(3) and plotted in Fig. 4(b) as a function of B, for both the zigzag and armchair configurations. The value of h is shown to be constant whatever B, even for values of B lower than the nanometer. A slight discrepancy (around 6%) is observed between the DFT and MS data, as expected due to the assumptions related to each method. Eqs. (3) and (4) describing the buckling in the framework of the continuum elastic theory are thus staying valid even for 2D materials provided

that a value for the thickness is considered appropriately. Finally, no effect of the graphene orientation, armchair or zigzag, on buckling is found to be significant in our numerical simulations, as also observed by MD simulations in [34]. Such a conclusion has also been numerically obtained by MD in the case of stretching/bending tests [32].

4. Discussion and conclusion

Most of the thickness values found in the literature for graphene are less than the interlayer spacing of 3.34 Å in graphite. These values correspond to an effective thickness, *i.e.* a thickness that is related to the elastic coefficients of the single graphene layer. In our study, an effective thickness of 0.91 Å has been determined by DFT in the framework of the elastic buckling of plates. The value h of the thickness has been found not to depend on the size of the buckle, in agreement with the average thickness determined in a previous work [39] by fitting the ϵ_c=f(B) curve obtained by MD. The in-plane rigidity of graphene has also been determined by DFT and found to be equal to $C_{xx} = 21.7\,\mathrm{eV/Å^2}$. Using $h = 0.91\,$Å in Eq. (6), a bending rigidity D equal to 1.49 eV has been calculated. This value is in good agreement with the one ($D = 1.41\,$eV) determined by DFT from the energy of carbon nanotubes with respect to the radius of curvature [40]. Concerning the results obtained using interatomic potentials, it is known that the REBO 2002 potential gives $C_{xx} = 289\,\mathrm{J.m^{-2}}$ and D=1.42 eV [39], leading to h=0.97 Å using Eq. (6), also in good agreement with our results. It confirms that the buckling of graphene can be well described in the framework of the continuum elastic theory by assuming an effective thickness. In our study, it has been shown that this effective thickness is constant whatever the size of the buckle, even at the nanometer scale, and found equal to 0.91 Å and 0.97 Å using DFT calculations and MS simulations, respectively.

On one hand, given that the effective thickness for graphene is known, the strain applied on graphene can be simply determined from the buckle morphology, *i.e.* from its deflection and its width. This approach is all the more interesting from a practical point of view since the effective thickness has been found to be constant whatever the width of the buckle. On the other hand, it is also believed that such a strategy can be used to determine the effective thickness of 2D materials from strain-controlled mechanical tests, giving relevant information on the mechanical properties to which the effective thickness is related.

Acknowledgments

This work was funded by the French National Research Agency program "Chacal"(ANR-19-CE08-0022-01) and pertains to the french government program "Investissements d'Avenir"(EUR INTREE, reference ANR-18-EURE-0010).

References

[1] G. Abadias, E. Chason, J. Keckes, M. Sebastiani, G. B. Thompson, E. Barthel, G. L. Doll, C. E. Murray, C. H. Stoessel, and L. Martinu. Review Article: Stress in thin films and coatings: Current status, challenges, and prospects. *J. Vac. Sci. Technol.*, 36(2):020801, 2018.

[2] Y. Ni, S. Yu, H. Jiang, and L. He. The shape of telephone cord blisters. *Nat. Commun.*, 8(1):14138, 2017.

[3] M.J. Cordill, D.F. Bahr, N.R. Moody, and W.W. Gerberich. Recent Developments in Thin Film Adhesion Measurement. *IEEE Trans. Device Mater. Reliab.*, 4(2):163–168, 2004.

[4] M.J. Cordill, F.D. Fischer, F.G. Rammerstorfer, and G. Dehm. Adhesion energies of Cr thin films on polyimide determined from buckling: Experiment and model. *Acta Mater.*, 58(16):5520–5531, 2010.

[5] B. Eren, L. Marot, G. Günzburger, P.-O. Renault, T. Glatzel, R. Steiner, and E. Meyer. Hydrogen-induced buckling of gold films. *J. Phys. D: Appl. Phys.*, 47(2):025302, 2014.

[6] A.G. Evans and J.W. Hutchinson. On the mechanics of delamination and spalling in compressed films. *Int. J. Solids Struct.*, 20(5):455–466, 1984.

[7] S. Grachev, C. Cuminatto, E. Søndergård, and E. Barthel. High-Throughput Optimization of Adhesion in Multilayers by Superlayer Gradient. *EPJ web conf.*, 1224:1224–FF10–22, 2009.

[8] J.-Y. Faou, S. Grachev, E. Barthel, and G. Parry. From telephone cords to branched buckles: A phase diagram. *Acta Mater.*, 125:524–531, 2017.

[9] S.-J. Yu, X.-F. Xiao, M.-G. Chen, H. Zhou, J. Chen, P.-Z. Si, and Z.-W. Jiao. Morphological selections and dynamical evolutions of buckling patterns in SiAlNx films: From straight-sided to telephone cord or bubble structures. *Acta Mater.*, 64:41–53, 2014.

[10] A.A Volinsky, N.R Moody, and W.W Gerberich. Interfacial toughness measurements for thin films on substrates. *Acta Mater.*, 50(3):441–466, 2002.

[11] M.-W. Moon, K.-R. Lee, K.H. Oh, and J.W. Hutchinson. Buckle delamination on patterned substrates. *Acta Mater.*, 52(10):3151–3159, 2004.

[12] S.-J. Yu, G. Parry, C. Coupeau, and L. Li. Pressure-induced transition from wavy circular to ring-shaped buckles. *Int. J. Solids Struct.*, 225:111053, 2021.

[13] G. Parry, C. Coupeau, J. Colin, A. Cimetière, and J. Grilhé. Buckling and post-buckling of stressed straight-sided wrinkles: experimental AFM observations of bubbles formation and finite element simulations. *Acta Mater.*, 52(13):3959–3966, 2004.

[14] J.W. Hutchinson, M.D. Thouless, and E.G. Liniger. Growth and configurational stability of circular, buckling-driven film delaminations. *AcM&M*, 40(2):295–308, 1992.

[15] J.W. Hutchinson and Z. Suo. Mixed Mode Cracking in Layered Materials. In *Advances in Applied Mechanics*, volume 29, pages 63–191. Elsevier, 1991.

[16] F. Foucher, C. Coupeau, J. Colin, A. Cimetière, and J. Grilhé. How Does Crystalline Substrate Plasticity Modify Thin Film Buckling? *Phys. Rev. Lett.*, 97(9):096101, 2006.

[17] C. Coupeau, J. Grilhé, E. Dion, L. Dantas de Morais, and J. Colin. Evidence of vacuum between buckled films and their substrates. *Thin Solid Films*, 518(18):5233–5236, 2010.

[18] S. Hamade, J. Durinck, G. Parry, C. Coupeau, A. Cimetière, J. Grilhé, and J. Colin. Effect of plasticity and atmospheric pressure on the formation of donut- and croissantlike buckles. *Phys. Rev. E*, 91(1):012410, 2015.

[19] G. Parry, J. Colin, C. Coupeau, F. Foucher, A. Cimetière, and J. Grilhé. Effect of substrate compliance on the global unilateral post-buckling of coatings: AFM observations and finite element calculations. *Acta Mater.*, 53(2):441–447, January 2005.

[20] C. Coupeau, R. Boijoux, Y. Ni, and G. Parry. Interacting straight-sided buckles: An enhanced attraction by substrate elasticity. *J. Mech. Phys. Solids*, 124:526–535, 2019.

[21] S. Žák, A. Lassnig, M. J. Cordill, and R. Pippan. Finite element-based analysis of buckling-induced plastic deformation. *J. Mech. Phys. Solids*, 157:104631, 2021.

[22] A. Lassnig, V. L. Terziyska, J. Zalesak, T. Jörg, D. M. Toebbens, T. Griesser, C. Mitterer, R. Pippan, and M. J. Cordill. Microstructural Effects on the Interfacial Adhesion of Nanometer-Thick Cu Films on Glass Substrates: Implications for Microelectronic Devices. *ACS Appl. Nano Mater.*, 4(1):61–70, 2021.

[23] J.-Y. Faou, G. Parry, S. Grachev, and E. Barthel. How Does Adhesion Induce the Formation of Telephone Cord Buckles? *Phys. Rev. Lett.*, 108(11):116102, 2012.

[24] G. H. Wells, T. Hopf, K. V. Vassilevski, E. Escobedo-Cousin, N. G. Wright, A. B. Horsfall, J. P. Goss, A. G. O'Neill, and M. R. C. Hunt. Determination of the adhesion energy of graphene on SiC(0001) via measurement of pleat defects. *Appl. Phys. Lett.*, 105(19):193109, 2014.

[25] R. Boijoux, G. Parry, and C. Coupeau. Buckle depression as a signature of Young's modulus mismatch between a film and its substrate. *Thin Solid Films*, 645:379–382, 2018.

[26] T. Jiang, R. Huang, and Y. Zhu. Interfacial Sliding and Buckling of Monolayer Graphene on a Stretchable Substrate. *Adv. Funct. Mater.*, 24(3):396–402, 2014.

[27] Z. Li, I. A. Kinloch, R. J. Young, K. S. Novoselov, G. Anagnostopoulos, J. Parthenios, C. Galiotis, K. Papagelis, C.-Y. Lu, and L. Britnell. Deformation of Wrinkled Graphene. *ACS Nano*, 9(4):3917–3925, 2015.

[28] Merijntje S. Bronsgeest, Nedjma Bendiab, Shashank Mathur, Amina Kimouche, Harley T. Johnson, Johann Coraux, and Pascal Pochet. Strain Relaxation in CVD Graphene: Wrinkling with Shear Lag. *Nano Lett.*, 15(8):5098–5104, 2015.

[29] M. Petrović, Je. T. Sadowski, A. Šiber, and M. Kralj. Wrinkles of graphene on Ir(1 1 1): Macroscopic network ordering and internal multilobed structure. *Carbon*, 94:856–863, 2015.

[30] T. Georgiou, L. Britnell, P. Blake, R. V. Gorbachev, A. Gholinia, A. K. Geim, C. Casiraghi, and K. S. Novoselov. Graphene bubbles with controllable curvature. *Appl. Phys. Lett.*, 99(9):093103, 2011.

[31] Y. Huang, J. Wu, and K. C. Hwang. Thickness of graphene and single-wall carbon nanotubes. *Phys. Rev. B*, 74(24):245413, 2006.

[32] J.-X. Shi, T. Natsuki, X.-W Lei, and Q.-Q. Ni. Equivalent Young's modulus and thickness of graphene sheets for the continuum mechanical models. *Appl. Phys. Lett.*, 104(22):223101, 2014.

[33] L. Wang, Q. Zheng, J. Z. Liu, and Q. Jiang. Size Dependence of the Thin-Shell Model for Carbon Nanotubes. *Phys. Rev. Lett.*, 95(10):105501, 2005.

[34] Q. Lu and R. Huang. Nonlinear mechanics of single-atomic-layer graphene sheets. *Int. J. Appl. Mech.*, 01(03):443–467, 2009.

[35] J. P. Perdew, K. Burke, and M. Ernzerhof. Generalized Gradient Approximation Made Simple. *Phys. Rev. Lett.*, 77(18):3865–3868, 1996.

[36] S. Plimpton. Fast Parallel Algorithms for Short–Range Molecular Dynamics. *J. Comput. Phys*, 117:1–19, 1995.

[37] D. W. Brenner, O. A. Shenderova, J. A. Harrison, S. J. Stuart, Boris Ni, and Susan B. S. A second-generation reactive empirical bond order (REBO) potential energy expression for hydrocarbons. *J. Condens. Matter Phys.*, 14(4):783–802, 2002.

[38] S. Timoshenko. *Theory of elastic stability.* McGraw-Hill, New York and London, 1961.

[39] Q. Lu, M. Arroyo, and R. Huang. Elastic bending modulus of monolayer graphene. *J. Phys. D*, 42(10):102002, 2009.

[40] K. Kudin, G. E. Scuseria, and B. Yakobson. C 2 F , BN, and C nanoshell elasticity from *ab initio* computations. *Phys. Rev. B*, 64(23), 2001.